HHS Public Access

Author manuscript

Retina. Author manuscript; available in PMC 2021 August 02.

Published in final edited form as:

Retina. 2020 April ; 40(4): 632–642. doi:10.1097/IAE.0000000000002434.

CHOROIDAL THICKNESS AND VASCULARITY VARY WITH DISEASE SEVERITY AND SUBRETINAL DRUSENOID DEPOSIT PRESENCE IN NONADVANCED AGE-RELATED MACULAR DEGENERATION

TIARNAN D. KEENAN, BM BCh, PhD[*], **BRANDON KLEIN, BS**[†], **ELVIRA AGRÓN, MA**[*], **EMILY Y. CHEW, MD**[*], **CATHERINE A. CUKRAS, MD, PhD**[*], **WAI T. WONG, MD, PhD**[†]

[*]Division of Epidemiology and Clinical Applications, National Eye Institute, National Institutes of Health, Bethesda, Maryland; [†]Unit on Neuron-Glia Interactions in Retinal Diseases, National Eye Institute, National Institutes of Health, Bethesda, Maryland.

Abstract

Purpose: To investigate how choroidal features vary with age-related macular degeneration (AMD) severity in early-intermediate disease.

Methods: One hundred fifty-one eyes of 151 participants >50 years with no to intermediate AMD were analyzed with enhanced depth imaging optical coherence tomography. Mean macular choroidal thickness (CT), choroidal vascular thickness (CV), and choroidal vascularity index (CVI) were determined, and statistical associations were calculated.

Results: Decreased CT and CV were associated with increased axial length (+30 and +14 μm/mm, respectively; $P < 0.0001$ each), whereas decreased CVI was associated with increased age (+0.1%/year; $P = 0.004$). Compared with eyes with no/early AMD (Group 0), eyes with large drusen without late AMD in the fellow eye (Group 1) showed increased CV and CVI (+22 μm, $P = 0.03$ and +2.2%, $P = 0.02$, respectively). However, eyes with large drusen and late AMD in the fellow eye (Group 2) resembled Group 0. Eyes with subretinal drusenoid deposits demonstrated lower mean CT/CV/CVI than Group 0 (−57 μm, $P = 0.02$; −31 μm, $P = 0.02$; −3.6%, $P = 0.007$).

Conclusion: Early AMD progression seems associated with biphasic alterations in choroidal dimensions, increasing during early drusen formation but decreasing thereafter. Subretinal drusenoid deposits are independently associated with marked reductions in all choroidal parameters. Changes in choroidal vascular anatomy may drive or reflect the pathobiology of AMD progression.

Reprint requests: Wai T. Wong, MD, PhD, Unit on Neuron-Glia Interactions in Retinal Diseases, National Eye Institute, National Institutes of Health, 6 Center Drive, 6/217 Bethesda, MD 20892; wongw@nei.nih.gov; Catherine A. Cukras, MD, PhD, Division of Epidemiology and Clinical Applications, National Eye Institute, National Institutes of Health, Bethesda, Maryland 20892; cukrasc@nei.nih.gov.

None of the authors has any conflicting interests to disclose.

Keywords

age-related macular degeneration; choroidal thickness; choroidal vascularity index; reticular pseudodrusen; subretinal drusenoid deposits

Age-related macular degeneration (AMD) is the leading cause of visual loss among older people in developed countries.[1] The progression of AMD is incompletely understood and involves a complex interplay between genetic and environmental risk factors.[2,3] Although AMD-related changes in the retina and retinal pigment epithelial (RPE) cells have been well described, the nature of parallel anatomical changes occurring in the underlying choroid and how these contribute to disease progression are less clear.[4,5] It has been hypothesized that vascular loss in the choroid may be an early step in AMD pathogenesis[6–8] and may be causally associated with pathological changes in the RPE and retina.[9]

The relative lack of knowledge regarding the role of the choroid in AMD arises from difficulties in visualizing the choroid using conventional fundus imaging and deriving outcome measures to characterize its anatomy. However, the advent of enhanced depth imaging optical coherence tomography (EDI-OCT) has improved clinical visualization of the choroid[10] and enabled a quantitative characterization. Although the overall thickness of the choroid in AMD has been measured and related to AMD status in multiple studies, the relationships reported between choroidal thickness (CT) and AMD disease severity have been varied and conflicting in some cases; some studies have described CT as being decreased in nonexudative AMD,[11–13] and others have found no significant differences from normal non-AMD controls.[14–21] Comparisons of CT in AMD eyes with late atrophic disease with control eyes have also not been in agreement.[16,22–24] These differences likely arise from variability of CT as a function of multiple person-specific (e.g., age, sex, and systemic health) and ocular factors (e.g., axial length),[25–28] underscoring the need to correct for these factors in multivariate analyses. In addition, the derivation of anatomical outcome measures additional to CT, particularly those describing the vascular spaces within the choroid, can more fully characterize choroidal vascular change. These new measures have been derived more recently using semiautomated segmentation of choroidal vascular and stromal tissue in EDI-OCT images[29,30] and may help distinguish between changes affecting the vasculature itself (e.g., choroidal vascular atrophy) versus those centered in the stromal component (e.g., choroidal stromal shrinkage or fibrosis).

Another source of variability in previous studies of the choroid may relate to the concurrent presence of subretinal drusenoid deposits (SDD) (or reticular pseudodrusen) in eyes at different levels of AMD severity. Recent studies have indicated that SDD presence may have a very marked influence on choroidal anatomy,[5,15,24,31–41] and a lack of its comprehensive ascertainment in control and AMD eyes, as well as the absence of its accounting in the analyses, may have lent variability to previous studies. For example, Thorell et al[24] observed that eyes with geographic atrophy (GA) and SDD had significantly decreased CT, compared with eyes with GA and no SDD, but that eyes with GA and no SDD did not have significantly different CT, compared with normal eyes or those with early AMD.

In this study, we performed a comprehensive cross-sectional analysis of multiple choroidal parameters in a large number of eyes categorized according to AMD severity, with detailed accompanying phenotypic information, and for which the presence or absence of SDD had been rigorously ascertained using multimodal fundus imaging. We focused on choroidal involvement in the early stages of AMD progression, and eyes with late disease (GA or exudative disease) were not included. To discover choroidal differences as a function of early AMD severity, we performed the following analyses: 1) characterization of multiple quantitative choroidal outcome measures, including those describing vascular versus stromal status, 2) stratification of study eyes according to concurrent SDD presence, and 3) rigorous multivariate analyses with correction for non–AMD-related factors that influence choroidal parameters. Our results enabled a description of the ocular and patient-based factors that are influential on three choroidal parameters and an elucidation of the AMD-related features that exert an effect on choroidal anatomy. Our findings provide a fuller picture of how the choroid may change structurally across AMD progression and the factors that can influence its change.

Methods

Study Population

The study population comprised a cohort of participants currently enrolled in an ongoing prospective longitudinal study of dark adaptation in AMD.[42] Participants were adults older than 50 years of age recruited from the eye clinic at the National Eye Institute, National Institutes of Health, Bethesda, MD, between May 2011 and July 2017. The inclusion and exclusion criteria for this study have been described previously[42]; participants with bilateral late AMD were excluded. Eligible participants were categorized into severity categories based on their retinal features. All participants were assessed for the presence of SDD (as described below), and those with SDD were placed into a single separate group (Group SDD), regardless of the presence of large drusen or fellow eye late status. The remaining participants without SDD were separated into categories of increasing AMD severity, based on the presence of large drusen (diameter ≥ 125 μm), late AMD, or both (Table 1). The control group, Group 0, consisted of participants without any large drusen or late AMD (choroidal neovascularization or central geographic atrophy [CGA]) in either eye. Group 1 comprised participants with large drusen in one or both eyes and no late AMD in either eye. Group 2 consisted of participants with large drusen in one eye and late AMD (either CGA or choroidal neovascularization) in the fellow eye. Only one eye of each participant was designated as the study eye, as described previously.[42] In participants with large drusen in one eye only, the eye with large drusen was the study eye. In participants with late AMD in one eye, the eye without late disease was the study eye. Study eyes consequently had either no or early AMD or otherwise contained large drusen without features of late AMD in the same eye. The study was approved by the Institutional Review Board of the National Institutes of Health, and the tenets of the Declaration of Helsinki were followed (identifier NCT01352975, www.clinicaltrials.gov). This research complied with the Health Portability and Accessibility Act. All participants provided informed consent after the nature and possible consequences of the study were explained.

Examination, Retinal Imaging and Dark Adaptation Testing

Participants underwent measurement of best-corrected visual acuity (BCVA) (using the Early Treatment Diabetic Retinopathy Study [ETDRS] chart), ophthalmoscopic examination, and retinal imaging, as described previously.[42] Color fundus photographs and fundus autofluorescence images were acquired with the TRC-50DX retinal camera (Topcon Medical Systems, Tokyo, Japan). Infrared reflectance, fundus autofluorescence images, and spectral domain (SD) OCT scans were acquired with the Heidelberg Spectralis (Heidelberg Engineering, Heidelberg, Germany). Enhanced depth imaging optical coherence tomography scans were acquired as a single horizontal B-scan (comprising 768 A-scans, average of 100 individual repeated B-scans) centered at the fovea with a scan length of 8.7 mm.

Grading of eyes for the presence or absence of SDD was performed, as described previously.[42] This comprised masked grading of color fundus photographs, fundus autofluorescence images, and infrared reflectance images from the study eyes by three independent graders trained to identify areas of SDD that extended over an area of >1 disk area on each imaging modality. For this and other AMD categorization, discordant grades were adjudicated in combined conference to achieve a final consensus grade. Dark adaptation was measured using a prototype of the AdaptDx dark adaptometer (MacuLogix, Hummelstown, PA). Details about the testing procedure have been described else-where.[43] The rod intercept time (RIT), as defined previously,[42] a measure of dark adaptation function in the study eye, was measured in minutes. Tests that did not reach the specified threshold by the end of the 40-minute test time were assigned an RIT of 40 minutes.

Measurement of Choroidal Parameters

Enhanced depth imaging optical coherence tomography scans for each study eye were downloaded from the Heidelberg Eye Explorer (HEYEX) software (Heidelberg Engineering) and imported into ImageJ (National Institutes of Health, Bethesda, MD). Manual segmentation of the choroid was performed over the subfoveal region measuring 6 mm (i.e., 3 mm either side of the fovea) using the “polygon tool” in ImageJ software. The boundary between the choroid and RPE/Bruch membrane was defined as the outer border of the hyperreflective line corresponding to the RPE/Bruch membrane complex. The boundary between the choroid and sclera was defined as the inner border of the hyporeflective line corresponding to the choroid–sclera junction; however, in cases where a hyporeflective band (corresponding to the suprachoroidal layer) was present, the inner border of the hyporeflective band was chosen.[44]

The outcome measures pertaining to choroidal vascular spaces within the segmented choroidal area were measured using image analysis. In ImageJ software, the Niblack autolocal threshold tool has previously been used to identify luminal and stromal areas within the choroid.[29,30,45] However, these reports have applied Niblack thresholding at a single scale, which has resulted in effective delineation of large choroidal vessels but poor resolution of the smaller choroidal capillaries. A multiscale Niblack binarization method was therefore developed to achieve high-quality segmentation of both small and large choroidal vessels. Original EDI-OCT images (Figure 1A) underwent local contrast enhancement (to account for uneven illumination of the choroid) and passage through an

edge-preserving bilateral filter, followed by normalization to reduce noise, before thresholding. The processed image (Figure 1B) was binarized twice using Niblack's method, with the thresholding parameters adjusted for separate optimization of the segmentation of 1) the small choroidal vessels (Figure 1C) and 2) the large choroidal vessels in Sattler's and Haller's layers (Figure 1D). The two thresholded images were added to yield a multiscale binarized image, which was then subjected to a despeckling filter (Figure 1E). White pixels were defined to represent space within the choroidal lumina and black pixels the surrounding choroidal stroma (Figure 1, E and F). The adequacy of the algorithm to segment both large and small choroidal lumina was manually checked after rendering; adjustment of thresholding and processing parameters was performed to optimize segmentation.

These image segmentation measures enabled the calculation of the following choroidal parameters: 1) mean macular CT was defined as the total area of all pixels (black and white) within the segmentation outlines of the choroid, divided by the length of retina assayed (central 6 mm); this measure, given in units of μm, reflects the thickness of the choroid (averaged across the horizontal aspect of the macula); 2) mean macular choroidal vascular (CV) thickness was defined as the area of white pixels (choroidal vascular spaces), divided by the length of retina assayed (same central 6 mm); this measure, given in units of μm, reflects the thickness of the intraluminal component of the choroid (averaged across the horizontal aspect of the macula); 3) choroidal vascularity index (CVI) was defined as the ratio of CV to CT, expressed as a percentage[45]; this quantity reflects the proportion of the thickness of the central 6 mm of choroid that comprises intraluminal space.

Statistical Analysis

Univariate analysis of data (separately for CT, CV, and CVI) was performed for each of the eight variables of interest: age, sex, smoking status (never vs. ever), axial length, lens status (phakic vs. pseudophakic), BCVA, RIT, and AMD status (scored as Group 0–2 or Group SDD). The analysis was performed using non-parametric statistics (Mann–Whitney U test) because CT, CV, and CVI did not demonstrate normal distributions. Significance was set at $P < 0.05$.

Multivariate analysis of data (again, separately for CT, CV, and CVI) was performed by general linear regression. In each case, variables that were significant in univariate analysis were included in the first multivariate model (Model A). Variables that were significant ($P < 0.05$) in Model A were included in the next multivariate model (Model B). Additional models (Models C, D, etc.) were constructed to check, one at a time, whether any variable excluded from Model B was significant on inclusion. For AMD status, pairwise comparisons were made for each group, with Group 0 as the reference group. The models took into account the multiple comparisons that are made between groups. Computation was performed using SAS software version 9.3 (SAS Inc, Cary, NC).

Results

Participant Demographics

One hundred fifty-four eyes of 154 participants were enrolled in the study. Of these, 3 eyes of 3 participants were excluded for the following reasons: in two eyes, EDI-OCT image segmentation of the choroid–sclera boundary could not be performed because of a markedly thickened choroid; in another eye, a clinical history of central serous chorioretinopathy was recorded. Hence, the final number subjected to primary analysis was 151 eyes of 151 participants. The demographic characteristics of the participants are shown in Table 1, and the ocular characteristics of study eyes are shown in Table 2. Axial length data were available in 107 of 151 eyes.

Association of Choroidal Thickness With Age-Related Macular Degeneration Status and Other Variables

Univariate analysis of CT was performed separately for each of the 8 variables for all 151 eligible participants. Age-related macular degeneration status was significantly associated with CT: Group SDD eyes demonstrated a significantly lower CT relative to Group 0 eyes (median 128 and 180 μm, respectively; $P = 0.003$). Choroidal thickness in Group 1 eyes was numerically but nonsignificantly higher than in Group 0 eyes (median 215 and 180 μm; $P = 0.07$). Choroidal thickness in Group 2 eyes was numerically similar and not significantly different than in Group 0 eyes (median 192 and 180 μm; $P = 0.68$). The other variables that had a significant association with CT were age (r = −0.32; $P < 0.0001$), axial length (r = −0.35; $P = 0.0002$), lens status (median 204 and 135 μm for phakic and pseudophakic eyes, respectively; $P < 0.0001$), BCVA (r = 0.25; $P = 0.002$), and RIT (r = −0.25; $P = 0.002$). Sex ($P = 0.60$) and smoking status ($P = 0.29$) were not associated.

Multivariate analysis of CT was performed by general linear regression using the subset of 107 study eyes with recorded axial length data (as this variable was significantly associated with CT in univariate analysis). From the results of statistical Model B, variables that were significantly associated with CT were AMD status, axial length, lens status, and BCVA. Additional statistical models constructed to ascertain whether any variable excluded from model B might be significantly associated on inclusion failed to reveal additional significant associations. The results for model B are shown in Table 3 and Figure 2A. Results for AMD status were similar to those obtained by univariate analysis: Group SDD eyes had a significantly lower CT than Group 0 eyes ($P = 0.02$). Choroidal thickness in Group 1 eyes was numerically but nonsignificantly higher than in Group 0 eyes ($P = 0.07$), whereas CT in Group 2 eyes was not significantly different than in Group 0 eyes ($P = 0.85$). The other variables that had a significant association with CT were axial length ($P < 0.0001$), lens status ($P = 0.02$), and BCVA ($P = 0.01$). Rod intercept time and age were not significantly associated with CT.

Association of Choroidal Vascular Thickness With Age-Related Macular Degeneration Status and Other Variables

Data for CV were analyzed in a similar way to those for CT. Univariate analysis of CV showed that AMD status was significantly associated with CV: Group 1 eyes demonstrated a

significantly higher CV relative to Group 0 eyes (median 103 and 82 μm, respectively; $P = 0.02$), whereas CV in Group 2 eyes was numerically similar and not significantly different to Group 0 eyes (median 93 and 82 μm; $P = 0.56$). Group SDD eyes had a significantly lower CV than Group 0 eyes (median 49 and 82 μm; $P = 0.001$). The other variables that had a significant association with CV were age ($r = -0.34$; $P < 0.0001$), axial length ($r = -0.32$; $P = 0.001$), lens status (median 98 and 64 μm for phakic and pseudophakic eyes, respectively; $P < 0.0001$), BCVA ($r = 0.24$; $P = 0.003$), and RIT ($r = -0.26$; $P = 0.002$). Sex ($P = 0.75$) and smoking status ($P = 0.24$) were not associated.

Multivariate analysis of CV using the subset of 107 study eyes with recorded axial length data (as this variable was significantly associated with CV in univariate analysis) showed associations with variables that were shared with those found for CT, that is, AMD status, axial length, lens status, and BCVA. The results for model B are shown in Table 4 and Figure 2B. Results for AMD status were similar to those obtained by univariate analysis: Group 1 eyes had a significantly higher CV than Group 0 eyes ($P = 0.03$), whereas CV in Group 2 was not significantly different to that in Group 0 ($P = 0.65$). Group SDD eyes had a significantly lower CV than Group 0 eyes ($P = 0.02$). The other variables that had a significant association with CV were axial length ($P < 0.0001$), lens status ($P = 0.03$), and BCVA ($P = 0.01$), but not RIT or age. Additional statistical models were constructed to ascertain whether any variable excluded from model B might be significantly associated when included but these alternative models did not reveal additional significant associations.

Association of Choroidal Vascularity Index With Age-Related Macular Degeneration Status and Other Variables

Univariate analysis of CVI revealed that AMD status was significantly associated with CVI: Group 1 eyes demonstrated a significantly higher CVI relative to Group 0 eyes (median 47.7 and 45.1%, respectively; $P = 0.001$), whereas CVI in Group 2 was not significantly different to that in Group 0 eyes (median 47.9 and 45.1%; $P = 0.21$), and had numerically similar mean values (45.4 and 44.5%). Group SDD eyes demonstrated a significantly lower CVI than Group 0 eyes (median 41.0 and 45.1%; $P = 0.01$). The other variables that had a significant association with CVI were age ($r = -0.33$; $P < 0.0001$), lens status (median 47.2 and 43.5% for phakic and pseudophakic eyes, respectively; $P = 0.001$), and RIT ($r = -0.23$; $P = 0.004$). Axial length ($P = 0.99$), BCVA ($P = 0.32$), sex ($P = 0.94$), and smoking status ($P = 0.25$) were not associated.

Multivariate analysis of CVI was performed using the full data set of 151 study eyes (as axial length was not significantly associated with CVI in univariate analysis). Interestingly, only age and AMD group were significantly associated with CVI (Table 5 and Figure 2C). As with the results from univariate analysis, Group 1 eyes had a significantly higher CVI relative to Group 0 eyes ($P = 0.02$), whereas CVI in Group 2 eyes was not significantly different than in Group 0 eyes ($P = 0.40$). Group SDD eyes had a significantly lower CVI than Group 0 eyes ($P = 0.007$). The only other variable that had a significant association with CVI was age ($P = 0.004$). Of note, CVI was not significantly associated with axial length, pseudophakia, or BCVA, in the way that CT and CV were; RIT was also not associated.

Association of Choroidal Parameters With Visual Acuity and Rod Intercept Time

To examine potential relationships between the three choroidal parameters and measures of visual function, values of CT, CV, and CVI were plotted against 1) BCVA and 2) RIT. Best-corrected visual acuity was positively correlated with CT (r = 0.25, $P = 0.002$) and with CV (r = 0.24, $P = 0.003$). However, there was no significant correlation between BCVA and CVI (r = 0.08, $P = 0.32$). Rod intercept time was negatively correlated with CT (r = −0.25, $P = 0.002$) and with CV (r = −0.26, $P = 0.002$). Rod intercept time was also negatively correlated with CVI (r = −0.23, $P = 0.004$).

Discussion

The purpose of this study was to perform a comprehensive analysis of multiple anatomical choroidal parameters in a large number of eyes with detailed phenotypic information including AMD status, presence or absence of SDD, and functional measures such as BCVA and dark adaptation data. Additional to previous analyses, which have been limited largely to the study of overall choroidal dimensions in the form of CT, we analyzed in parallel with CT the outcome measures of CV and CVI, correlating each to AMD disease severity in a large patient cohort.[45] We included in our analyses patient and ocular data to identify factors other than AMD severity that were associated with CT/CV/CVI; correcting for these factors in multivariate analyses enabled us to relate choroidal outcome measures more specifically to AMD severity.

Comparing the results of our analyses for each choroidal parameter, we found that CT and CV exhibited largely congruent patterns of association, whereas CVI displayed some distinct associations. In particular, we found that CT and CV were both negatively correlated with axial length, consistent with the notion that axial elongation of the globe stretches and thins multiple ocular tissue layers[46,47] across both the myopic and hyperopic spectrum.[25–28,48] By contrast, CVI did not vary significantly with axial length, similar to a report by Agrawal et al,[45] indicating it as a descriptor of choroidal vascular status that is more robust to variations in ocular shape. The association between decreased CVI and SDD presence suggests that SDD may confer a loss of choroidal vascular status that is more pathological than the decreased CT induced by simple axial elongation as in high myopia. Subretinal drusenoid deposits presence may be linked to AMD-related processes involving 1) choroidal damage (e.g., choriocapillaris endothelial cell death, vessel hyalinization, and altered stromal extracellular matrix with fibrosis); 2) dysfunction in other neighboring tissue layers (particularly the RPE and Bruch membrane); and 3) the onset of choroidal thinning late in life, well after the period of ocular growth, in the background of decreased homeostatic reserve of the aged eye. Also, while previous studies have negatively correlated CT with increasing age,[25–28,45] we did not find this association for CT or CV. Choroidal vascularity index, however, was significantly and negatively correlated with increasing age. Hence, CVI may have potential use as an outcome measure for aging and disease processes that preferentially affect the choroidal vasculature versus the stromal component.

Our analysis of how the three choroidal parameters varied with increasing AMD severity suggested that, compared with Group 0, they are increased in Group 1 but not in Group 2. Hence, in contrast to many reports suggesting that the choroid may undergo monotonic

thinning or remain unchanged during AMD progression, our novel findings here indicate that changes in the choroid may in fact be biphasic during disease progression. In the first phase, CV and CVI may increase over time during earlier stages of AMD development; in the second phase, as disease progresses, changes in the choroid may result in decreased CV and CVI. We hypothesize that the first phase might represent a compensatory stage during drusen accumulation and early localized choriocapillaris loss or otherwise an initial engorgement of the vasculature induced by early inflammatory changes in the choroid accompanying the onset of drusen formation. We are aware of just one previous study reporting increased CT in AMD, as part of the Beijing Eye Study,[49] although the generalizability of this previous study to non-Asian populations is uncertain. In the Beijing Eye Study, CT was increased in intermediate AMD but not late AMD. However, this study did not account for SDD presence and measured CT at single points rather than CT/CV/CVI across the macular zone. As such, our observations add to the notion that early increases in choroidal vascular status can occur in AMD before later degenerative changes accrue.

Processes that lead to marked and significant losses of CT and vascular thickness seem to be present in eyes with SDD; in our analysis, these eyes demonstrate the lowest mean values for CT, CV, and CVI, which were all significantly lower than for the other severity groups. Although decreased CT in eyes with SDD has been previously reported,[5,15,24,31–41] our findings additionally uncover that SDD eyes demonstrate a disproportionately greater loss in choroidal vascular thickness, even as the overall choroid thins, resulting in a significantly reduced CVI. We discovered that, although SDD and large soft drusen are often found together in eyes in the SDD group, the effect of SDD presence on choroidal parameters predominates that, pertaining to the presence or absence of large drusen, an influence also observed for its association with impaired dark adaptation.[42] For these reasons, in analyses of choroidal parameters according to AMD severity, it is crucial to stratify according to the presence or absence of SDD.

Few previous reports have examined potential differences in CVI according to AMD status severity. Consistent with our findings, Corvi et al[15] observed significantly lower CVI (as well as CT and CV) in 18 eyes with SDD (and no soft drusen), compared both with 18 eyes with early AMD (and no SDD) and with 18 healthy control eyes. Unlike our study, this analysis did not perform adjustment for age or axial length, did not include eyes with intermediate AMD, and excluded eyes where SDD coexisted with soft drusen. We are aware of one report examining CVI (alongside CT) in eyes with SDD, in the context of intermediate AMD.[31] These authors observed significantly lower CT and CV in eyes with SDD. Choroidal vascularity index (assessed using swept-source OCT en face slabs over a 6-mm diameter macular circle) was numerically lower in eyes with SDD, but the difference was not statistically significant ($P = 0.06$). Potential reasons for the lack of statistical significance (unlike in the current study) include a lower threshold for assignment of SDD presence in the previous study (where a single SDD lesion on SD-OCT alone was sufficient for a positive SDD grading in any eye) and the lack of multiscale binarization. One additional report analyzed CT and CVI according to SDD presence in 50 eyes with a broad range of AMD severity, potentially comprising the full spectrum of nonexudative AMD.[34] The authors observed significantly lower CT and CVI (assessed using swept-source OCT en face slabs) in eyes with SDD (graded by multimodal imaging). However, the CVI metric in

this previous study pertained to large choroidal vessels only (as the upper boundary of the highest choroidal slab was 40 μm below Bruch membrane), and no multivariable analysis was performed.

In addition, we have examined here the relationship between choroidal parameters and visual function. Multivariate analysis found significant positive correlations between BCVA and CT and CV, but not CVI. However, the range of BCVA in this study population was small, and extrapolations between CT and visual acuity per se are limited. Interestingly, RIT was not associated with any of the three parameters in multivariate analysis. As such, taking these findings together, we did not find here that choroidal parameters exerted large and direct effects on measures of visual function in this study population.

The strengths of this study include the detailed phenotypic characterization of the study population, allowing for stratification of the SDD phenotype. Additional strengths come from the comprehensive analysis of cross-sectional choroidal parameters using EDI-OCT, including CT, CV, and CVI, all of which were assessed over the width of the macula (rather than at a single subfoveal point). Potential limitations in this study were the presence of missing axial length data in approximately one-third of study eyes. Interestingly, CVI was not associated with axial length, permitting use of the full data set in the analysis of this parameter. In addition, the resolution of EDI-OCT imaging was likely insufficient in revealing the complete vascular anatomy of the choroid and may not have revealed very small vessels that did not display evident hyporeflective centers. The resolution of the images was also insufficient for accurate segmentation of the choroid into sublayers (i.e., small vessel layer, Sattler's layer, and Haller's layer) to enable CV and CVI to be calculated for subregions within the choroid.

In conclusion, we performed a comprehensive assessment of multiple EDI-OCT–derived choroidal outcome measures, which permit a broader description of choroidal status in AMD eyes. Our results reinforce the significance of SDD presence as a strong factor associated with choroidal attenuation in the form of lower CT, CV, and CVI. In eyes without SDD, all three choroidal parameters changed with increasing AMD severity in a biphasic manner, with an initial increase associated with drusen formation that was more evident in the parameters of CV and CVI than with CT alone. Future longitudinal analyses that track choroidal vascular parameters in individual eyes over multiple stages of AMD progression would be helpful to support the potentially dynamic nature of choroidal changes with disease progression. Three-dimensional anatomical mapping of the choroid using high-resolution imaging in AMD populations may also be useful in localizing pathological changes to subregions/sublayers of the choroid. Taken together, the findings here support the notion that structural changes in the choroid occur in the progression of early and intermediate AMD, and that these warrant closer scrutiny in considerations of AMD pathobiological mechanisms.

Acknowledgments

Supported by the National Eye Institute Intramural Research Program. The sponsor or funding organization had no role in the design or conduct of this research. T. D. Keenan was partly funded by an award from the Bayer Global Ophthalmology Awards Program.

References

1. Congdon N, O'Colmain B, Klaver CC, et al. Causes and prevalence of visual impairment among adults in the United States. Arch Ophthalmol 2004;122:477–485. [PubMed: 15078664]
2. Fritsche LG, Igl W, Bailey JN, et al. A large genome-wide association study of age-related macular degeneration highlights contributions of rare and common variants. Nat Genet 2016;48:134–143. [PubMed: 26691988]
3. Fritsche LG, Fariss RN, Stambolian D, et al. Age-related macular degeneration: genetics and biology coming together. Annu Rev Genomics Hum Genet 2014;15:151–171. [PubMed: 24773320]
4. Chirco KR, Sohn EH, Stone EM, et al. Structural and molecular changes in the aging choroid: implications for age-related macular degeneration. Eye 2017;31:10–25. [PubMed: 27716746]
5. Spaide RF. Disease expression in nonexudative age-related macular degeneration varies with choroidal thickness. Retina 2018;38:708–716. [PubMed: 28505013]
6. Whitmore SS, Sohn EH, Chirco KR, et al. Complement activation and choriocapillaris loss in early AMD: implications for pathophysiology and therapy. Prog Retin Eye Res 2015;45:1–29. [PubMed: 25486088]
7. Zeng S, Whitmore SS, Sohn EH, et al. Molecular response of chorioretinal endothelial cells to complement injury: implications for macular degeneration. J Pathol 2016;238:446–456. [PubMed: 26564985]
8. Seddon JM, McLeod DS, Bhutto IA, et al. Histopathological insights into choroidal vascular loss in clinically documented cases of age-related macular degeneration. JAMA Ophthalmol 2016;134:1272–1280. [PubMed: 27657855]
9. Mullins RF, Khanna A, Schoo DP, et al. Is age-related macular degeneration a microvascular disease? Adv Exp Med Biol 2014;801:283–289. [PubMed: 24664709]
10. Spaide RF, Koizumi H, Pozzoni MC. Enhanced depth imaging spectral-domain optical coherence tomography. Am J Ophthalmol 2008;146:496–500. [PubMed: 18639219]
11. Esmaeelpour M, Kajic V, Zabihian B, et al. Choroidal Haller's and Sattler's layer thickness measurement using 3-dimensional 1060-nm optical coherence tomography. PLoS One 2014;9: e99690. [PubMed: 24911446]
12. Sigler EJ, Randolph JC. Comparison of macular choroidal thickness among patients older than age 65 with early atrophic age-related macular degeneration and normals. Invest Ophthalmol Vis Sci 2013;54:6307–6313. [PubMed: 23982844]
13. Lee JY, Lee DH, Lee JY, Yoon YH. Correlation between subfoveal choroidal thickness and the severity or progression of nonexudative age-related macular degeneration. Invest Ophthalmol Vis Sci 2013;54:7812–7818. [PubMed: 24204054]
14. Broadhead GK, Hong T, McCluskey P, et al. Choroidal thickness and microperimetry sensitivity in age-related macular degeneration. Ophthalmic Res 2017;58:27–34. [PubMed: 28427081]
15. Corvi F, Souied EH, Capuano V, et al. Choroidal structure in eyes with drusen and reticular pseudodrusen determined by binarisation of optical coherence tomographic images. Br J Ophthalmol 2017;101:348–352. [PubMed: 27190128]
16. Yiu G, Chiu SJ, Petrou PA, et al. Relationship of central choroidal thickness with age-related macular degeneration status. Am J Ophthalmol 2015;159:617–626. [PubMed: 25526948]
17. Jonas JB, Forster TM, Steinmetz P, et al. Choroidal thickness in age-related macular degeneration. Retina 2014;34:1149–1155. [PubMed: 24220257]
18. Wood A, Binns A, Margrain T, et al. Retinal and choroidal thickness in early age-related macular degeneration. Am J Ophthalmol 2011;152:1030–1038 e2. [PubMed: 21851922]
19. Kim SW, Oh J, Kwon SS, et al. Comparison of choroidal thickness among patients with healthy eyes, early age-related maculopathy, neovascular age-related macular degeneration, central serous chorioretinopathy, and polypoidal choroidal vasculopathy. Retina 2011;31:1904–1911. [PubMed: 21878855]
20. Manjunath V, Goren J, Fujimoto JG, Duker JS. Analysis of choroidal thickness in age-related macular degeneration using spectral-domain optical coherence tomography. Am J Ophthalmol 2011;152:663–668. [PubMed: 21708378]

21. Chung SE, Kang SW, Lee JH, Kim YT. Choroidal thickness in polypoidal choroidal vasculopathy and exudative age-related macular degeneration. Ophthalmology 2011;118:840–845. [PubMed: 21211846]
22. Adhi M, Liu JJ, Qavi AH, et al. Choroidal analysis in healthy eyes using swept-source optical coherence tomography compared to spectral domain optical coherence tomography. Am J Ophthalmol 2014;157:1272–1281 e1. [PubMed: 24561169]
23. Lindner M, Bezatis A, Czauderna J, et al. Choroidal thickness in geographic atrophy secondary to age-related macular degeneration. Invest Ophthalmol Vis Sci 2015;56:875–882. [PubMed: 25587059]
24. Thorell MR, Goldhardt R, Nunes RP, et al. Association between subfoveal choroidal thickness, reticular pseudodrusen, and geographic atrophy in age-related macular degeneration. Ophthalmic Surg Lasers Imaging Retina 2015;46:513–521. [PubMed: 26057754]
25. Tan KA, Gupta P, Agarwal A, et al. State of science: choroidal thickness and systemic health. Surv Ophthalmol 2016;61:566–581. [PubMed: 26980268]
26. Ooto S, Hangai M, Yoshimura N. Effects of sex and age on the normal retinal and choroidal structures on optical coherence tomography. Curr Eye Res 2015;40:213–225. [PubMed: 25153829]
27. Abbey AM, Kuriyan AE, Modi YS, et al. Optical coherence tomography measurements of choroidal thickness in healthy eyes: correlation with age and axial length. Ophthalmic Surg Lasers Imaging Retina 2015;46:18–24. [PubMed: 25559504]
28. Barteselli G, Chhablani J, El-Emam S, et al. Choroidal volume variations with age, axial length, and sex in healthy subjects: a three-dimensional analysis. Ophthalmology 2012;119:2572–2578. [PubMed: 22921388]
29. Sonoda S, Sakamoto T, Yamashita T, et al. Choroidal structure in normal eyes and after photodynamic therapy determined by binarization of optical coherence tomographic images. Invest Ophthalmol Vis Sci 2014;55:3893–3899. [PubMed: 24894395]
30. Sonoda S, Sakamoto T, Yamashita T, et al. Luminal and stromal areas of choroid determined by binarization method of optical coherence tomographic images. Am J Ophthalmol 2015;159:1123–1131 e1. [PubMed: 25790737]
31. Lains I, Wang J, Providencia J, et al. Choroidal changes associated with subretinal drusenoid deposits in age-related macular degeneration using swept-source optical coherence tomography. Am J Ophthalmol 2017;180:55–63. [PubMed: 28579063]
32. Masuda N, Kojima M, Yamashita M, et al. Choroidal structure determined by binarizing optical coherence tomography images in eyes with reticular pseudodrusen. Clin Ophthalmol 2017;11:791–795. [PubMed: 28490860]
33. Yun C, Ahn J, Kim M, et al. Ocular perfusion pressure and choroidal thickness in early age-related macular degeneration patients with reticular pseudodrusen. Invest Ophthalmol Vis Sci 2016;57:6604–6609. [PubMed: 27926751]
34. Zheng F, Gregori G, Schaal KB, et al. Choroidal thickness and choroidal vessel density in nonexudative age-related macular degeneration using swept-source optical coherence tomography imaging. Invest Ophthalmol Vis Sci 2016;57:6256–6264. [PubMed: 27849311]
35. Alten F, Heiduschka P, Clemens CR, Eter N. Longitudinal structure/function analysis in reticular pseudodrusen. Invest Ophthalmol Vis Sci 2014;55:6073–6081. [PubMed: 25146989]
36. Ueda-Arakawa N, Ooto S, Ellabban AA, et al. Macular choroidal thickness and volume of eyes with reticular pseudodrusen using swept-source optical coherence tomography. Am J Ophthalmol 2014;157:994–1004. [PubMed: 24491418]
37. Haas P, Esmaeelpour M, Ansari-Shahrezaei S, et al. Choroidal thickness in patients with reticular pseudodrusen using 3D 1060-nm OCT maps. Invest Ophthalmol Vis Sci 2014;55:2674–2681. [PubMed: 24651554]
38. Spaide RF. Outer retinal atrophy after regression of subretinal drusenoid deposits as a newly recognized form of late age-related macular degeneration. Retina 2013;33:1800–1808. [PubMed: 23764969]

39. Garg A, Oll M, Yzer S, et al. Reticular pseudodrusen in early age-related macular degeneration are associated with choroidal thinning. Invest Ophthalmol Vis Sci 2013;54:7075–7081. [PubMed: 24071958]
40. Querques G, Querques L, Forte R, et al. Choroidal changes associated with reticular pseudodrusen. Invest Ophthalmol Vis Sci 2012;53:1258–1263. [PubMed: 22222508]
41. Switzer DW Jr, Mendonca LS, Saito M, et al. Segregation of ophthalmoscopic characteristics according to choroidal thickness in patients with early age-related macular degeneration. Retina 2012;32:1265–1271. [PubMed: 22222760]
42. Flamendorf J, Agron E, Wong WT, et al. Impairments in dark adaptation are associated with age-related macular degeneration severity and reticular pseudodrusen. Ophthalmology 2015; 122:2053–2062. [PubMed: 26253372]
43. Jackson GR, Edwards JG. A short-duration dark adaptation protocol for assessment of age-related maculopathy. J Ocul Biol Dis Infor 2008;1:7–11. [PubMed: 20072631]
44. Yiu G, Pecen P, Sarin N, et al. Characterization of the choroid-scleral junction and suprachoroidal layer in healthy individuals on enhanced-depth imaging optical coherence tomography. JAMA Ophthalmol 2014;132:174–181. [PubMed: 24336985]
45. Agrawal R, Gupta P, Tan KA, et al. Choroidal vascularity index as a measure of vascular status of the choroid: measurements in healthy eyes from a population-based study. Sci Rep 2016;6:21090. [PubMed: 26868048]
46. Grossniklaus HE, Green WR. Pathologic findings in pathologic myopia. Retina 1992;12:127–133. [PubMed: 1439243]
47. Fujiwara T, Imamura Y, Margolis R, et al. Enhanced depth imaging optical coherence tomography of the choroid in highly myopic eyes. Am J Ophthalmol 2009;148: 445–450. [PubMed: 19541286]
48. Chen FK, Yeoh J, Rahman W, et al. Topographic variation and interocular symmetry of macular choroidal thickness using enhanced depth imaging optical coherence tomography. Invest Ophthalmol Vis Sci 2012;53:975–985. [PubMed: 22232433]
49. Zhao J, Wang YX, Zhang Q, et al. Macular choroidal small-vessel layer, Sattler's layer and Haller's layer thicknesses: the Beijing Eye Study. Sci Rep 2018;8:4411. [PubMed: 29535365]

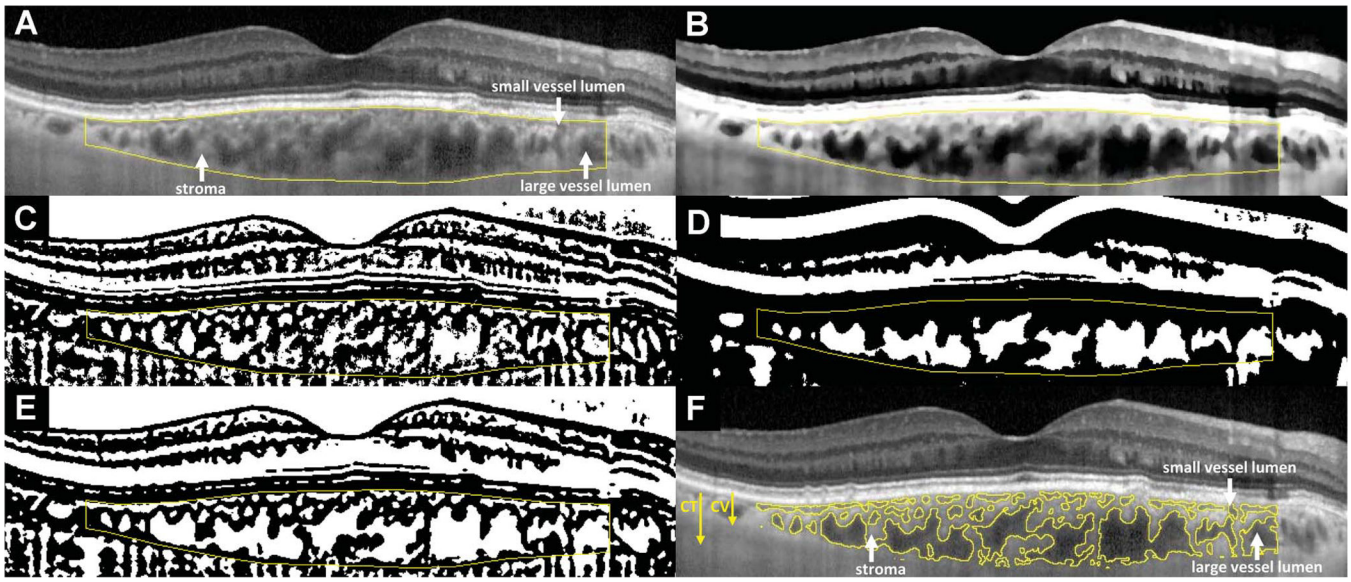

Fig. 1.

Choroidal segmentation algorithms used for the analysis of EDI-OCT images to calculate choroidal parameters. Horizontally oriented EDI-OCT B-scans traversing the center of the fovea were analyzed. Manual segmentation of the inner and outer borders of the choroid (**A**) was performed over the central 6-mm zone (3 mm on either side of the foveal center). These segmentation lines outlining the overall dimensions of the choroid were used in the computation of CT. For the segmentation of individual vascular spaces in cross-section from the nonvascular stroma, the original EDI-OCT image first underwent contrast enhancement, passage through a bilateral filter, and normalization to produce the processed image (**B**). Image binarization was performed once on the processed image for an optimized segmentation of small choroidal vessels using the Niblack autolocal threshold tool (**C**). A second separate image binarization procedure was performed on the processed image for a differently optimized segmentation of large choroidal vessels using Niblack thresholding with altered parameters (**D**). The two binarized images were then combined to produce a multiscale image, which underwent additional despeckling (**E**). This eventual image was then segmented into areas with contiguous black or white pixels, with the segments containing white pixels representing vascular luminal spaces, and the segments containing black pixels representing nonvascular choroidal stroma (**F**). Choroidal thickness arrow: CT, in μm, was defined as the total area of all pixels (black and white) within the segmentation outlines of the choroid, divided by the length of retina assayed (central 6 mm). CV arrow: CV thickness (in μm) was defined as the area of all white pixels (choroidal vascular spaces), divided by the length of retina assayed (central 6 mm). Hence, CT (all pixels) = CV (white pixels) + choroidal stromal thickness (black pixels). Choroidal vascularity index was defined as the ratio CV:CT, expressed as a percentage.

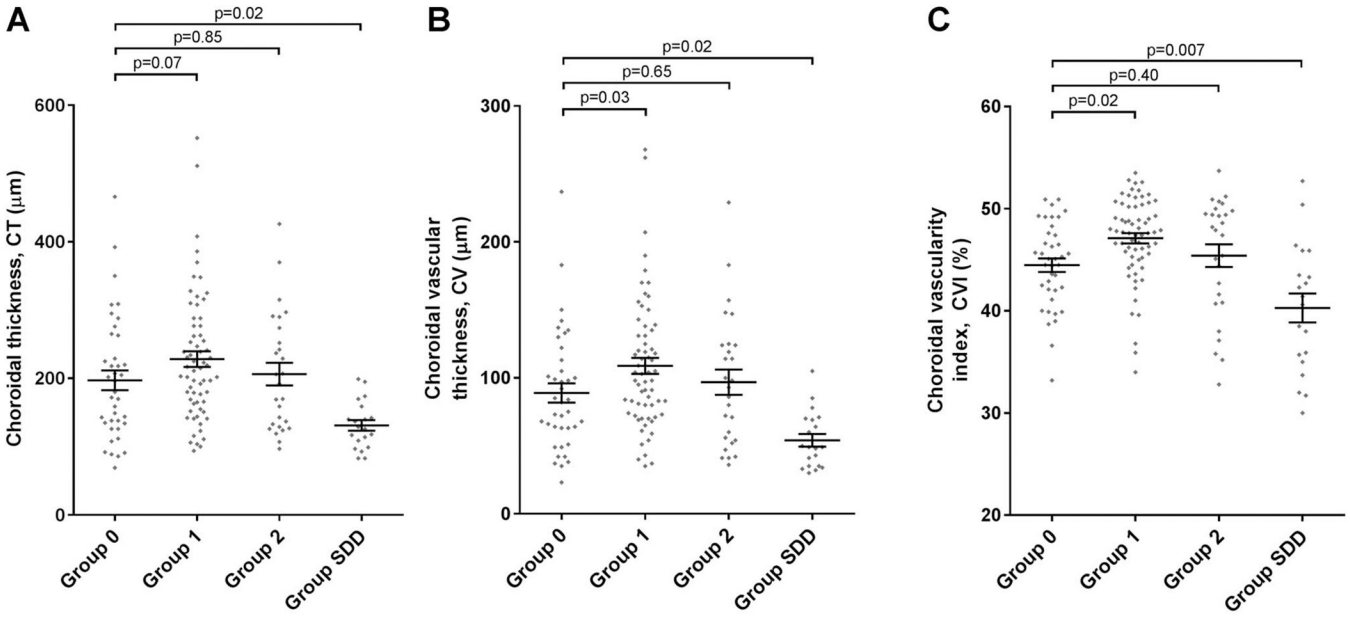

Fig. 2.

Analysis of choroidal parameters according to AMD severity group: (**A**) CT; (**B**) CV; (**C**) CVI. Comparisons were made between eyes in Group 0 (study eyes with no AMD or early AMD) and those in Group 1 (study eyes with large drusen, where the fellow eye had no late AMD), Group 2 (study eyes with large drusen, where the fellow eye had late AMD), and Group SDD (study eyes with subretinal drusenoid deposits). The horizontal lines and the error bars represent the mean and standard error of the distribution, respectively. The *P* values shown were obtained by multivariate analysis using general linear regression.

Table 1.

Definition of Study Age-Related Macular Degeneration Severity Categories and Demographic Characteristics of Study Participants Analyzed (n = 151) in Each Group

AMD Severity Category	Definition		Patient Characteristics			
	Study Eye	Fellow Eye	N (% of Total)	Mean Age (SD), years	Male Sex, No. (%)	Ever Smoked, No. (%)
Group 0	No or only small/medium drusen (≤125 μm diameter)	No or only small/medium drusen (≤125 μm diameter)	39 (25.8%)	73.1 (9.1)	15 (38.5)	17 (43.6)
Group 1	Large drusen (>125 μm diameter)	Absence of late AMD (CGA or NVAMD)	65 (43.0%)	69.9 (9.9)	35 (53.8)	31 (47.7)
Group 2	Large drusen (>125 μm diameter)	Late AMD (CGA or NVAMD)	27 (17.9%)	73.5 (8.6)	10 (37.0)	14 (51.9)
Group SDD	Presence of SDD, no late AMD	All possible phenotypes	20 (13.2%)	78.4 (7.1)	7 (35.0)	10 (50.0)
Total			151	72.5 (9.5)	67 (44.4)	72 (47.7)

NVAMD, neovascular age-related macular degeneration.

Table 2.

Ocular Characteristics of Study Eyes (n = 151) According to AMD Severity Group Assignment

	Group 0: Eyes With No AMD or Early AMD	Group 1: Eyes With Large Drusen; No Late AMD in FE	Group 2: Eyes With Large Drusen; Late AMD in FE	Group SDD: Eyes With Subretinal Drusenoid Deposits	Total
N	39	65	27	20	151
Mean BCVA (SD), no. of letters	85.3 (5.2) (≈Snellen 20/20)	82.5 (5.6) (≈Snellen 20/25)	79.0 (8.6) (≈Snellen 20/25)	80.3 (6.2) (≈Snellen 20/25)	82.3 (6.6) (≈Snellen 20/25)
Phakic status, pseudophakic no. (%)	13 (33.3)	12 (18.5)	8 (29.6)	12 (60.0)	45 (29.8)
Mean axial length (SD), mm	24.6 (1.6); n = 24	24.3 (1.2); n = 45	24.0 (0.9); n = 23	24.0 (1.1); n = 15	24.2 (1.2); n = 107
Mean rod intercept time (SD), minutes	13.5 (5.4)	20.1 (10.4)	24.9 (11.6)	39.1 (2.0)	21.8 (11.8)

FE, fellow eye.

Table 3.

Results of Multivariate Analysis of Choroidal Thickness (CT); n = 107 Study Eyes With Axial Length Recorded

Parameter	Choroidal Thickness (μm)			
	Estimate	95% Confidence Limits		*P*
Axial length	−29.8	−41.4	−18.1	<0.0001
Pseudophakia	−42.7	−77.9	−7.5	0.02
BCVA (letters)	2.9	0.6	5.3	0.01
AMD Group 1 vs. Group 0	36.4	−2.4	75.2	0.07
AMD Group 2 vs. Group 0	4.1	−41.0	49.3	0.85
AMD Group SDD vs. Group 0	−56.9	−106.4	−7.4	0.02
Age				ns
Sex				ns
Smoking status				ns
RIT				ns

Table 4.

Results of Multivariate Analysis of CV Thickness; n = 107 Study Eyes With Axial Length Recorded

Parameter	Choroidal Vascular Thickness (μm)			
	Estimate	95% Confidence Limits		*P*
Axial length	−14.4	−20.5	−8.3	<0.0001
Pseudophakia	−21.0	−39.4	−2.6	0.03
BCVA (letters)	1.6	0.4	2.8	0.01
AMD Group 1 vs. Group 0	22.2	1.9	42.5	0.03
AMD Group 2 vs. Group 0	5.4	−18.2	28.9	0.65
AMD Group SDD vs. Group 0	−30.9	−56.7	−5.0	0.02
Age				ns
Sex				ns
Smoking status				ns
RIT				ns

Table 5.

Results of Multivariate Analysis of CVI; n = 151 Study Eyes

Parameter	CVI (%)			
	Estimate	95% Confidence Limits		*P*
Age	−0.12	−0.21	−0.04	0.004
AMD Group 1 vs. Group 0	2.24	0.36	4.12	0.02
AMD Group 2 vs. Group 0	0.99	−1.31	3.29	0.40
AMD Group SDD vs. Group 0	−3.55	−6.11	−0.98	0.007
Sex				ns
Smoking status				ns
Axial length				ns
Pseudophakia				ns
BCVA				ns
RIT				ns